Shear Excitation of Gravity Waves. Part II: Upscale Scattering from Kelvin–Helmholtz Waves

G. CHIMONAS

Georgia Institute of Technology, Atlanta, GA 30332

J. R. GRANT

Gould Defense Systems, Inc., Middletown, RI 02840

(Manuscript received 6 February 1984, in final form 18 June 1984)

ABSTRACT

Upscale scattering of Kelvin–Helmholtz waves to gravity shear waves involves the nonlinear interaction of two Kelvin–Helmholtz waves with wavenumbers k and k' to produce a wave with wavenumber $k - k'$. Calculations show that the process produces long-wavelength radiating gravity waves in atmospheric conditions that favor the Kelvin–Helmholtz instabilities. Both line and continuum evaluations are presented in the context of the unstable tropospheric jet. It is shown that even when the unstable shear in the jet is confined to a shallow sublayer, producing markedly small-scale Kelvin–Helmholtz instabilities, upscale scattering to the large-scale waves is an efficient process.

1. Introduction

Mesoscale wave activity has been observed to result from instability of wind fields (Herron and Tolstoy, 1969; Hooke *et al.*, 1973; Hooke and Hardy, 1975; Keliher, 1975). Similarly, smaller scale waves and clear air turbulence have been associated with local wind shear (Metcalf and Atlas, 1973).

A quantitative description of this dynamic instability usually begins with some form of inviscid linearized theory. This has proven rather successful. Many of the observed wave characteristics agree well with predictions of the formulation (Merrill, 1977; Mastrantonio *et al.*, 1976). On deeper scrutiny, however, some difficulties are found. These concern the coexistence of the gravity shear and the Kelvin–Helmholtz wave instabilities. The gravity shear waves are obtained in numerical studies of continuously stratified wind profiles (Lalas and Einaudi, 1976; Mastrantonio *et al.*, 1976; Davis and Peltier, 1976; see also the overreflection calculations of Jones, 1968; Rosenthal and Lindzen, 1983). These, and numerous subsequent studies, find that in linearized inviscid theory the unstable wind field can support a sequence of growing wave types. The shortest wavelength species is the classical Kelvin–Helmholtz wave spectrum. Invariably it contains the fastest growing waves, and imposes the least demands on the flow fields. It first appears at Richardson numbers that are too high for any development of the other wave types. The other types form a sequence of families with increasing wavelengths, decreasing growth rates and more exacting demands on the flow profiles. We shall refer to all these non-Kelvin–Helmholtz waves as gravity shear wave instabilities.

When the simple model flows of the earlier studies are replaced with profiles that are closer to the observed atmospheric states, the dominance of the Kelvin–Helmholtz waves increases. Field measurements show that the wind field is unstable (Richardson numbers less than 0.25) over very restricted height intervals (Merrill, 1977; Metcalf and Atlas, 1973). When calculations are performed using such unstable sublayers, the Kelvin–Helmholtz waves are found to have growth rates that are orders of magnitude greater than the gravity shear waves (Chimonas and Grant, 1984).

All this suggests that the Kelvin–Helmholtz modes are the only ones that could reach significant amplitudes before nonlinear modifications of the mean flow prevent any further development through the linear instability mechanism (Davis and Peltier, 1979; Fritts, 1982). The inclusion of viscosity in the linearized theory only amplifies this conclusion (Davis and Peltier, 1977).

Consequently, although linear stability theory provides a satisfactory definition of the wave characteristics observed for gravity shear waves, it is unlikely tht such waves are produced by the linear instability mechanism.

This peculiarity could be resolved by showing that nonlinear interactions generate gravity shear waves with many of the characteristics of the linearized modes. This paper describes such a nonlinear model,

in which interactions among the growing Kelvin–Helmholtz waves force the co-production of gravity shear waves. Because the gravity shear waves are an atmospheric response to the forcing fields, they reflect the characteristics of the medium: hence the appearance of wave parameters closely related to the linearized modal (stability) analysis.

The theory is a weakly nonlinear formulation, in that the gravity shear wave response is not considered significant to the evolution of the Kelvin–Helmholtz waves. Of course, the Kelvin–Helmholtz waves could be strongly influenced by other nonlinear processes such as vortex pairing, resonant triad scattering across the short wavelength spectrum, vortex rollup, overturning, and cascade to turbulence. However, this does not directly enter the physics of the gravity shear wave generation. The formulation only requires a finite amplitude spectrum of some given form. It does, however, affect the calculations of the generation efficiency, since this requires explicit forms for all the wave fields. This work evaluates forcing functions using the fields of linearized stability theory to represent the Kelvin–Helmholtz waves. Our own view is that in this context the linearized fields provide accurate results.

The model produces a gravity shear wave with wavenumber K from the nonlinear interaction between two Kelvin–Helmholtz waves with wavenumbers k and $(-k + K)$. It is understood that k is at least an order of magnitude greater than K, so there is a very real difference in characteristics of the gravity shear and Kelvin–Helmholtz wave types. It appears that the use of such interactions in geophysical fluid dynamics originated with Longuet-Higgins (1950), who was concerned with microseisms: "continuous oscillations of the ground . . . which are recorded by all sensitive seismographs and are not due to earthquakes or to local causes such as rain, traffic or gusts of wind." Microseisms are generated by storms over the oceans, and were recognized to be linked, somehow, with the surface wave activity of the storms. However, a surface wave with horizontal wavenumber k damps out vertically as $\exp\{-k\partial\}$, where ∂ is depth below the ocean surface, and so it is impossible for the wind-generated surface waves on a deep ocean to significantly excite disturbances at the ocean bed, at least directly. However, Longuet-Higgins recognized that two surface waves, one with wavenumber k, the other with wavenumber $(-k + \Delta)$, have a nonlinear interaction that excites the mode with wavenumber Δ. Also, as $\Delta \to 0$, this nonlinear response penetrates to the great depths necessary to transmit a seismic pressure disturbance to the ocean floor. In the present context, the wavenumber differencing of close members of the Kelvin–Helmholtz family allows excitation of the much longer wavelength gravity shear waves.

The approach is an analytical formulation. Fritts (1982) developed a numerical model of this process in the atmosphere, but the studies are complementary. The numerical work allows a more sophisticated description of the evolution of the wave fields and the mean flow, and can be extended to include competing mechanisms that might influence the basic scattering process (Fritts, 1983).

This work isolates the upscale scattering from other nonlinear features, and studies some special details. Thus the mean wind in the atmosphere is allowed to contain small scale vertical shears superimposed on the tropospheric jet. Such secondary scales allow shear instabilities without violating the general trend of parameters revealed by radiosondes, but they also create similarly small scale Kelvin–Helmholtz waves. The upscale scattering to the gravity shear wave spectrum thus involves two classes of waves with totally different spatial scales. The present calculations show that the interaction nevertheless proceeds efficiently. The calculations also show why the gravity shear modes of linearized theory appear as the response to the Kelvin–Helmholtz excitations, explaining the "agreement" between observations and linearized theory.

The analysis investigates the relationship between idealized line models and the continuum theory. In a line model, the Kelvin–Helmholtz spectrum is confined to two pre-selected lines (delta functions in a k space representation) that can scatter to the gravity shear wave regime. Much theoretical and numerical wave work is confined to line approximations, although the atmosphere presents a continuum situation. The present upscale scattering model can be efficient in the continuum situation if the Kelvin–Helmholtz packet is the correct size.

In all, the model suggests that a physically significant gravity shear wave component can accompany the development of Kelvin–Helmholtz waves. The conditions for efficient line forcing are exactly the same as those required for gravity shear wave instabilities of the flow, but the time scale for appearance of the gravity shear waves is much shorter through the nonlinear mechanism. The continuum scattering is efficient under further restrictions.

2. The vortex pairing mechanism

It has been pointed out by McIntyre and Weissman (1978) and Davis and Peltier (1979) that under some circumstances scattering from Kelvin–Helmholtz waves to gravity shear waves can proceed through vortex pairing. This is known to be important for the evolution of the finite amplitude Kelvin–Helmholtz wave packet (Scotti and Corcos, 1972; Patnaik *et al.*, 1976). It involves a wavelength doubling of a shear instability by resonant interaction with its subharmonic. When the Kelvin–Helmholtz spectrum is very close in wavenumber space to the gravity shear wave spectrum, it may well lead to a significant upscale

transfer of energy (but see Fritts, 1983). The vortex pairing mechanism is distinct from the interaction considered in this paper in two respects. First, we are considering upscale scattering from Kelvin–Helmholtz waves to very much longer wavelengths, rather than just wavelength doubling. Second, our upscale scattering to the gravity shear waves is weakly nonlinear but does not discount other strong nonlinearities within the Kelvin–Helmholtz subsystem. The vortex pairing calculations (Davis and Peltier, 1979) involve a strong coupling feedback between the Kelvin–Helmholtz wave and its subharmonic, but discount other interactions that may influence the time evolution of the Kelvin–Helmholtz waves.

3. Formulation of the upscale scattering

The gravity shear waves arise as a response of the atmosphere to forcing effects provided by the Kelvin–Helmholtz waves. We will calculate this response using a linearized response theory. The forcing derives from a specific subset of the terms describing the nonlinear interactions between waves of the Kelvin–Helmholtz spectrum. This subset will be isolated from all other nonlinear terms, and its effects alone computed. In principle, the Kelvin–Helmholtz fields may themselves result from highly nonlinear processes. The formulation given below is perfectly general in this regard.

Let (x, y, z) be a right-handed set of cartesian coordinates aligned to the gravitational acceleration $-\hat{z}g$. Let p represent pressure, ρ density, $\mathbf{V}$ velocity and C the speed of sound. The equations of motion describing the atmosphere are taken to be

$$\rho \frac{D\mathbf{V}}{Dt} + \nabla p - \rho \mathbf{g} = 0, \tag{3.1}$$

$$\frac{D\rho}{Dt} + \rho \nabla \cdot \mathbf{V} = 0, \tag{3.2}$$

$$\frac{Dp}{Dt} - C^2 \frac{D\rho}{Dt} = 0, \tag{3.3}$$

where the Lagrangian time derivative

$$\frac{D}{Dt} = \frac{\partial}{\partial t} + \mathbf{V} \cdot \nabla \tag{3.4}$$

has been used. It is not really necessary to use more than an incompressible Boussinesq approximation of this set.

Let the fields be resolved into a mean part, a Kelvin–Helmholtz part, and a gravity shear wave part; these will be denoted by subscripts 0, 1 and 2, respectively. For instance,

$$\mathbf{V} = \mathbf{V}_0 + \mathbf{V}_1 + \mathbf{V}_2. \tag{3.5}$$

This separation can be made by identifying the various components within a Fourier representation, but in the present model the distinct horizontal scales allow an immediate separation in real space. Although the two procedures are essentially equivalent, the real space separation offers a more convenient and transparent formulation. The set of equations can be linearized in the gravity shear wave amplitudes, since it is assumed that this component does not introduce significant feedbacks into the evolution of the system.

Then, the same basis that allowed separation of the fields into three components now allows each equation to be partitioned into groups of terms with distinct scales. This yields an equation set for each wave type. For the gravity shear wave component this results in

$$\rho_0\left[\left(\frac{\partial}{\partial t} + \mathbf{V}_0 \cdot \nabla\right)\mathbf{V}_2 + \mathbf{V}_2 \cdot \nabla \mathbf{V}_0\right] + \nabla p_2 - \rho_2 \mathbf{g} = \mathbf{F}_2 = -\rho_0 \mathbf{V}_1 \cdot \nabla \mathbf{V}_1, \tag{3.6}$$

$$\left(\frac{\partial}{\partial t} + \mathbf{V}_0 \cdot \nabla\right)\rho_2 + \mathbf{V}_2 \cdot \nabla \rho_0 = 0, \tag{3.7}$$

$$\left(\frac{\partial}{\partial t} + \mathbf{V}_0 \cdot \nabla\right)(p_2 - C_0^2 \rho_2) + \mathbf{V}_2 \cdot \nabla p_0 - C_0^2 \mathbf{V}_2 \cdot \nabla \rho_0 = Q_2 = -\mathbf{V}_1 \cdot \nabla p_1 + C_0^2 \mathbf{V}_1 \cdot \nabla \rho_1. \tag{3.8}$$

The terms on the right-hand sides are nonlinear products of Kelvin–Helmholtz fields which scatter into the gravity shear wave. Some smaller terms have been dropped, as they can be shown to make contributions that are of order $(c_x/C)^2$ relative to those retained. Here, c_x is the horizontal phase speed of the Kelvin–Helmholtz wave, so the approximation is highly accurate for most situations encountered in the atmosphere.

4. Line theory and formulation

Many nonlinear wave calculations use a line interaction approximation. That is, the continuous spectra in wavenumber space that represent the real functions are replaced by a few discrete lines located at strategic points in k space. This approach has the merit of greatly simplifying the calculations while illustrating important features of the interactions. It is often possible to extend such calculations into quantitative measures of the interaction. In this section we investigate upscale scattering of Kelvin–Helmholtz waves by using a line approximation. Later, these results are used in evaluating the continuum situation. Regardless of the choice between lines or continua, explicit forms are needed for the expressions that appear on the right-hand sides of (3.6)–(3.8). These forcing functions are composed of quadratic products of Kelvin–Helmholtz fields. The atmospheric Kelvin–Helmholtz waves go through a life cycle of growth, strong nonlinear interaction, and eventual decay and disappearance as their environment becomes unsup-

portive. Here we are concerned with the gravity wave response, not the mechanics of Kelvin–Helmholtz excitations. Ideally, these required functions would be available to use from field measurements, but this is not the case and so some model for them must be adopted.

An approach that should yield sensible results can be based on the Kelvin–Helmholtz fields of linearized stability theory. The forcing fields of line theory are obtained by choosing a Kelvin–Helmholtz system

$$w_1 = \hat{z}\cdot\mathbb{V}_1 = A_k q_k(z)\exp(\sigma t + i\omega t - ikx) + A_{k'} q_{k'}(z)\exp(\sigma' t + i\omega' t - ik'x) + \text{c. c.}, \quad (4.1)$$

where σ, σ', ω, ω', k and k' are all real.

All other field components of this system—pressure, density, and so forth—are obtained from (4.1) by using the relationships of linearized theory. In this way the terms within the nonlinear products are completely defined, and it only remains to extract the part of them that forces the gravity shear wave scales; this is easily accomplished. Any second-order product of the Kelvin–Helmholtz fields defined from (4.1) will contain one of the two exponential forms

$$\exp[(\sigma + \sigma')t + i(\omega + \omega')t - i(k + k')x], \quad (4.2)$$

$$\exp[(\sigma + \sigma')t + i(\omega - \omega')t - i(k - k')x]. \quad (4.3)$$

The wavenumbers in the upscale scattering are chosen so that

$$k = k' + \text{del}, \quad (4.4)$$

where

$$|\text{del}/k| \ll 1. \quad (4.5)$$

With this restriction, the factor (4.3) corresponds to a wavenumber that is very much smaller than those of the Kelvin–Helmholtz fields. The wavenumber in (4.2) corresponds to the first harmonic of the Kelvin–Helmholtz waves. Only the smaller wavenumbers (4.3) can possibly be appropriate to the gravity shear waves, and so only terms with this factor will be retained. The separation del will be matched to the scale of the gravity shear waves of the background atmosphere.

If the forcing wavenumber $(k - k')$ matches the wavenumber of some gravity shear mode, the forcing frequency $(\omega - \omega')$ will also closely match the frequency of the mode. This follows from the general result that the shear instabilities all have more or less the same horizontal phase speed, matching the background wind speed near the height of the minimum Richardson number. This matching between the parameters of the free modes and the parameters of the forcing terms suggests the possibility of a resonant response, and, to some extent, the calculated response depends on this enhancement. But the growth terms $\exp(\sigma + \sigma')t$ prevent any exact resonance, the response is nonsingular, and, as far as we can determine, the linearized response theory is always valid. If $(\sigma + \sigma')$ is allowed to be very small, exact resonance is possible. However, the primary goal of this paper is to show that a significant gravity wave component accompanies the rapid onset of the Kelvin–Helmholtz waves, and so $(\sigma + \sigma')$ will always be too large to allow this special situation.

When the amplitudes A_k, $A_{k'}$ in (4.1) are specified, (3.6)–(3.8) becomes a fully deterministic set of equations for the response fields $(\rho_2, p_2, \mathbb{V}_2)$.

The forcing terms in (3.6)–(3.8) depend on t and x only through a common exponential factor

$$\exp[(\sigma + \sigma')t + i(\omega - \omega')t - i(k - k')x].$$

Consequently, this is the t- and x-dependence of the response fields. Their amplitudes and z-dependences can be discovered through a Green's function technique as follows.

Equations (3.6)–(3.8) are reduced to a single equation in just one of the field components. It is most convenient to work with a density-weighted form of the vertical velocity field w:

$$w_2(x, z, t) = \rho_0^{-1/2}\phi_2(z)\exp[(\sigma + \sigma')t + i(\omega - \omega')t - i(k - k')x]. \quad (4.6)$$

The function ϕ_2 is goverened by the inhomogeneous second-order perfect differential equation

$$\phi_2'' + [J\beta\alpha_2^2\Omega_2^{-2} + U''\alpha_2\Omega_2^{-1} - \alpha_2^2]\phi_2 = E_2(q_k, q_{k'}), \quad (4.7)$$

where $E_2(q_k, q_{k'})$ is a complicated nonlinear function of the Kelvin–Helmholtz fields. It is given in detail in the Appendix.

The left-hand side of (4.7) is simply the left-hand side of the Taylor–Goldstein equation, so if E_2 is set to zero the linearized stability problem for gravity shear waves is recovered. The notation follows Part I of this study (Chimonas and Grant, 1984, this issue). Briefly, velocities are scaled with a characteristic speed V; lengths are scaled to a tropospheric scale H;

$$\alpha_2 = (k - k')H \quad (4.8)$$

is a nondimensionalized wavenumber;

$$\Omega_2 = \{[(\omega - \omega') - i(\sigma + \sigma')]H/V\} - \alpha_2 U \quad (4.9)$$

is a nondimensionalized intrinsic frequency;

$$J = gH/V^2 \quad (4.10)$$

is a characteristic Richardson number;

$$\beta J = -g(\rho_0'/\rho_0 - p_0'/\gamma p_0)(H/V^2) \quad (4.11)$$

is the nondimensionalized Brunt–Väisälä frequency squared;

$$U = \hat{x}\cdot\mathbb{V} \quad (4.12)$$

is the mean wind on the x direction; and a prime denotes a derivative with respect to nondimensionalized height

$$y = z/H. \quad (4.13)$$

The boundary conditions for solutions of (4.7) are that $\phi_2(0)$ and $\phi_2(\infty)$ are both zero.

Formally, the solution of (4.7) is now expressed through a Green's function. Let ϕ_+ and ϕ_- be solutions of

$$\phi'' + [J\beta\alpha_2^2\Omega_2^{-2} + U''\alpha_2\Omega_2^{-1} - \alpha_2^2]\phi = 0, \quad (4.14)$$

obeying the upper and lower boundary conditions, respectively. Then

$$\phi_2(y) = \int_0^\infty dy' G(y, y') E_2[q_k(y'), q_{k'}(y')], \quad (4.15)$$

where

$$G(y, y') = [\phi_+(y)\phi_-(y')H(y - y') + \phi_-(y)\phi_+(y')H(y' - y)]\mathcal{W}^{-1}(\phi_-, \phi_+). \quad (4.16)$$

The Heaviside function H is equal to 1 for positive arguments and zero for negative arguments. The Wronskian is defined as

$$\mathcal{W}(\phi_-, \phi_+) = \phi_+\phi_-' - \phi_-\phi_+'. \quad (4.17)$$

It can be evaluated at any convenient height, since it is independent of y. Wherever (4.14) has an eigensolution, that is a function ϕ_M obeying both boundary conditions, the system degenerates to

$$\phi_+ = \phi_- = \phi_M, \quad (4.18)$$

$$\mathcal{W}(\phi_M, \phi_M) = 0, \quad (4.19)$$

an exact resonance which causes G and ϕ_2 to become infinite. This will never happen in the present model, which is concerned with fast-growing modes scattering into that part of the spectrum where the growth rate is much lower. Thus the forcing frequency $[\omega - \omega' + i(\sigma + \sigma')]$ and forcing wavenumber $(k - k')$ will not constitute an eigenvalue set for (4.14). However, these forcing parameters may be sufficiently close to eigenvalues to produce a noticeably enhanced response. That is, $\mathcal{W}$ may be so small that the response ϕ_2 is significant (observable) for very moderate amplitudes of the Kelvin–Helmholtz forcing fields.

This is found to happen; it is then useful to relate the response amplitude to the degree of mismatch between the forcing parameters and the nearest resonance, as follows. The wavenumbers are always chosen so that the scattered wavenumber $(k - k')$ lies in the domain of the gravity shear modes. Then the mismatch between the parameters of forcing and modes can be regarded as a mismatch of the frequencies. If the gravity shear mode with wavenumber $(k - k')$ has frequency $(i\sigma_M + \omega_M)$, the frequency difference between mode and forcing, Δ, given by

$$\Delta = i\sigma_M + \omega_M - [i(\sigma + \sigma') + (\omega - \omega')], \quad (4.20)$$

indicates closeness to resonance. Obviously, $\Delta = 0$ gives $\mathcal{W} = 0$ and exact resonance.

5. Numerical results

Although the theoretical formulation is relatively direct, the numerical evaluations are complex and time consuming. The stability characteristics of a flow must be determined in both the Kelvin–Helmholtz and gravity shear wave regimes. The Kelvin–Helmholtz eigenfunctions must be found and stored, together with the functions ϕ_+ and ϕ_- needed for the Green's functions; then the overlap integrals of (4.15) must be computed.

The flow used in this study is a tropospheric jet with some small scale shear structure providing subcritical Richardson numbers. Its precise form and stability characteristics are described in detail in Part I. A composite of the Kelvin–Helmholtz/gravity shear wave stability boundaries is shown in Fig. 1.

For line interactions, two Kelvin–Helmholtz modes k and k' are selected as the basis for all the calculations described above. There are infinitely many ways of making the wavenumber choices, and we have sought to display a characteristic set of such results.

It is appropriate to give special weight to the fastest growing Kelvin–Helmholtz waves. Therefore, the first calculations used two Kelvin–Helmholtz lines, k and k', in the region of maximum growth rate, and arranged their separation $(k - k')$ to fall in the spectral range of the gravity shear waves. The nonlinear calculations for the forced gravity wave response were performed. Then with $(k - k')$ kept fixed (i.e., a constant wavelength for the forced wave), a scan was made across the Kelvin–Helmholtz spectrum (k, k') with a sequence of line calculations. This allows a study of forcing efficiency as the wave matching parameters, especially $|\Delta|$, change. The entire set of

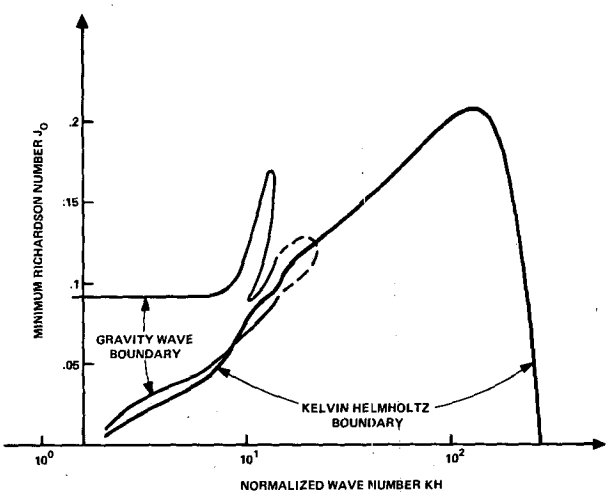

FIG. 1. Stability boundaries for the tropospheric jet used in this study. Instabilities are found at all points inside the designated boundaries. The Kelvin–Helmholtz waves dominate for wavenumbers kH greater than ~20, and extend out to $kH = 275$.

calculations can be repeated for different wavelengths ($k - k'$) of gravity shear waves and various mean flow configurations.

In all calculations the amplitudes of the two lines, $A_k e^{\sigma t}$ and $A_{k'} e^{\sigma' t}$ [Eq. (4.1)], must be chosen. We have always normalized so that each of them provides a maximum vertical velocity of 0.1 m s^{-1} in the linear theory. Since these factors are common to all fields in the problem, no further separate specifications of t or A are needed.

The response is measured by computing the maximum in the field of the vertical velocity component of the forced disturbance. Figures 2 and 3 show scans through the allowed range of Kelvin–Helmholtz waves for two choices of the forced wavenumber. It is evident that the "second-order" long wavelength amplitude is considerably greater than the primary first-order amplitudes. This reflects the efficiency of the upscaling interaction, because the 0.1 m s^{-1} assumed for the short wavelength seems very reasonable. Note that for every factor of 2 by which these forcing amplitudes increase, the response is enhanced by a factor of 4. It may also be added that for the large scale modes the horizontal flow velocity is an order of magnitude greater than the vertical velocity, while for the Kelvin–Helmholtz waves the two components are about equal. Thus the ratio of vertical components used in Figs. 2 and 3 downplays the upscaling efficiency.

The trends in Figs. 2 and 3 confirm that the forcing becomes more effective as $|\Delta| \to 0$ and resonance is approached. However, the amplitude of Δ is controlled by the growth rates σ entering (4.3) and it is greatest when the Kelvin–Helmholtz waves consist of the

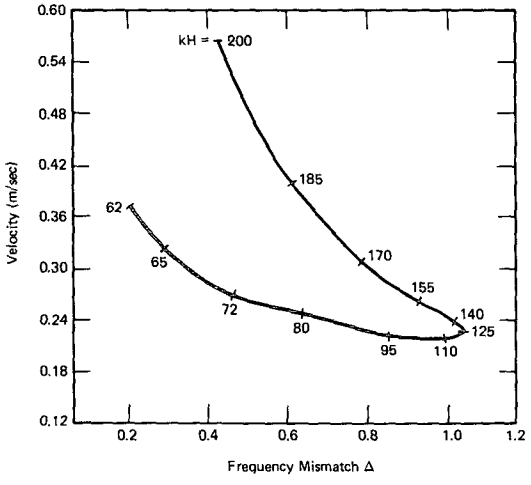

FIG. 2. Amplitude of the gravity shear waves with (normalized) wavenumber $KH = 13$ forced by two Kelvin–Helmholtz waves with wavenumbers k and $(k - K)$. The domain of Kelvin–Helmholtz wave space k is scanned from $kH = 60 \to 200$. The response is related to the mismatch from resonance Δ. Calculation performed for $H = 12$ km, flow parameter $J_0 = 0.16$.

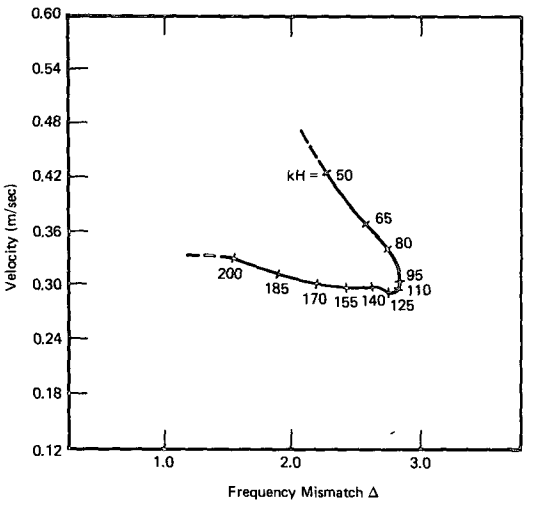

FIG. 3. As in Fig. 2 but with $KH = 7$ and $J_0 = 0.075$.

fastest growing pair. This local minimum of the response must be balanced against the maximum of the Kelvin–Helmholtz amplitudes expected in this region.

Nonlinear processes limit the amplitudes that instabilities can attain. In effect, the growth rate of a mode is not a constant but decreases toward zero as maximum wave amplitude is approached. Any decrease in the forcing growth rate ($\sigma + \sigma'$), however, enhances the response factor for upscale cascade to the long wavelengths. We conclude that the response factors calculated here probably underestimate the upscaling efficiency. Far more complex calculations will be needed to determine a realistic form for the *final* amplitudes of either long- or short-wavelength disturbances. The present calculations show that upscale scattering can be a very efficient process during the growth phase of instabilities.

Figures 4 and 5 compare the forced response in one of our calculations with the nearest long-wavelength eigenmode. For a resonance the two would be identical. However, the much larger growth rate ($\sigma + \sigma'$) associated with the forced field has a marked effect on the profile shape, and the response cannot be identified as a modal field. Superimposed on Fig. 4 is a schematic of the typical primary Kelvin–Helmholtz wave involved in these calculations. There is a tremendous mismatch in the two types of wave scales, yet the nonlinear scattering proves to be highly effective. Figures 6 and 7 compare the two-dimensional phase patterns of the eigenmode and the forced response. Again, the differences result from the greatly different time scales for growth. The forced mode shows a stronger radiating character in the uppermost domains. This feature was noted in the numerical work of Fritts (1982). It derives from the time delay between response in the far field and the amplitude

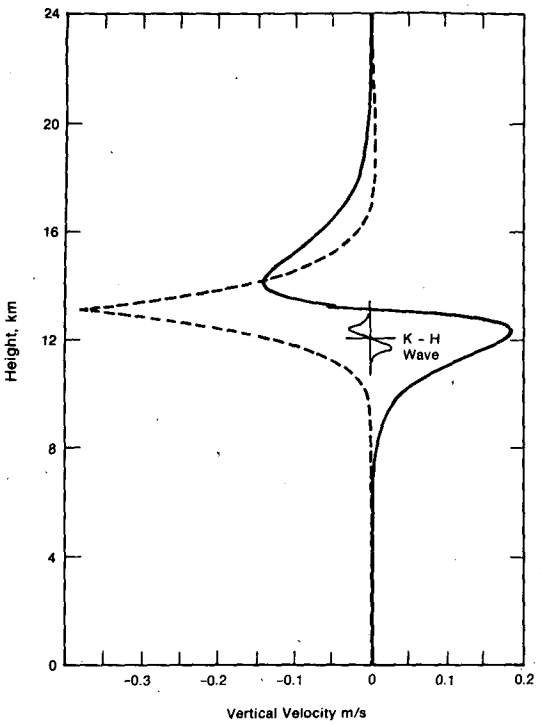

FIG. 4. The z-dependence of the gravity shear mode with normalized wavenumber $KH = 9$ in the flow with $J_0 = 0.075$. The mode has phase speed 0.56 and growth rate 0.003. Real and imaginary parts of the wave are shown separately. Schematic around 13 km gives relative vertical scales of the Kelvin–Helmholtz waves.

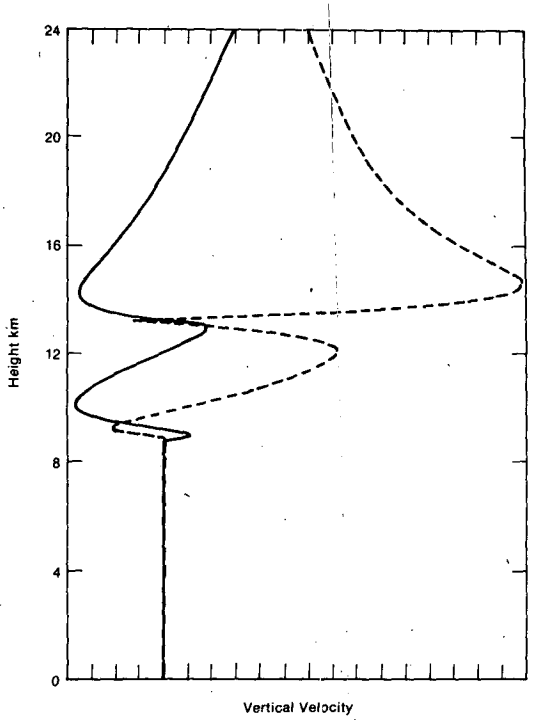

FIG. 5. The z-dependence of the forced gravity wave with normalized wavenumber $KH = 9$ in the flow with $J_0 = 0.075$. Forcing was provided by two Kelvin–Helmholtz waves with the largest growth rates that allowed matching of the wavenumber. The combined growth rate ($\sigma + \sigma'$) was 2.55 and phase speed $(\omega + \omega')/K$ was 0.56. Compare with the gravity mode profile of Fig. 4. Real and imaginary parts of the wave function are shown.

of the forcing function. Accordingly, the higher (more distant) the field, the smaller its amplitude. The radiating phase character is necessary for the upward transmission of energy that allows the field at a given altitude to grow in time.

6. Wavenumber selection

The scattering efficiency demonstrated in the previous section resulted from a judicious selection of wavenumbers. Some further discussion is called for.

Two selection processes are involved. First, the Kelvin–Helmholtz spectrum will be dominated by the wavenumbers that have the largest growth rates. The growth rate curves of the Kelvin–Helmholtz waves are flat about their apexes, so this is not a severely restrictive consideration. Second, the response function favors those long-wavelength disturbances that result in small values of $\mathcal{W}$. This is a more effective selection process, and can be related to the predictions of linearized stability theory.

It has been noted previously that in the full frequency/wavenumber domain, $\mathcal{W}$ has zeros wherever the natural modes exist. Figure 1 shows that these modes form a limited continuum in wavenumber space. Correspondingly, $\mathcal{W}$ is zero over a range of small wavenumbers K_M with associated eigenfrequencies $\omega_M + i\sigma_M$. For any Kelvin–Helmholtz wave with

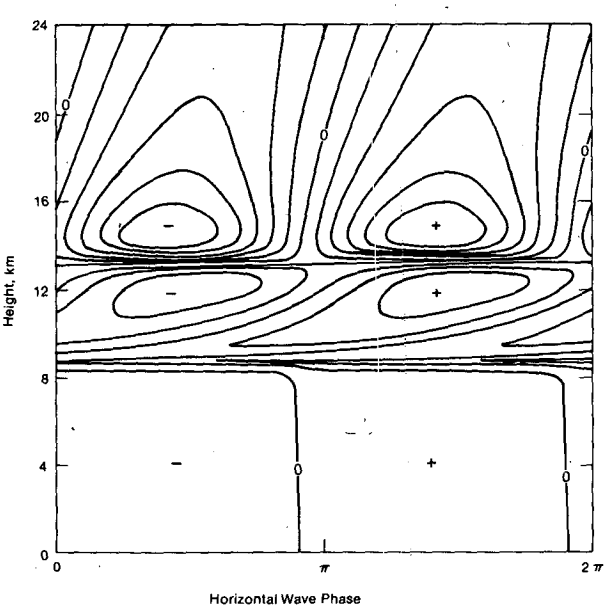

FIG. 6. Two-dimensional phase structure of the mode discussed in Fig. 4.

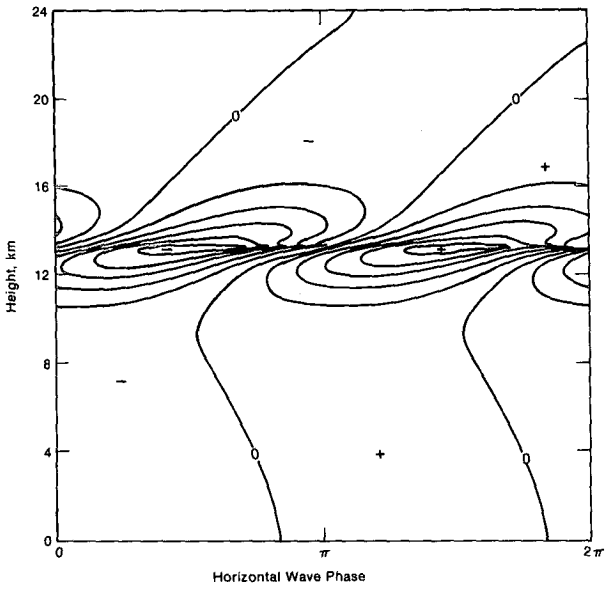

FIG. 7. Two-dimensional phase structure of the forced gravity wave described in Fig. 5.

wavenumber k and a significant growth rate, it is possible to locate a continuum of k', all with large growth rates, and all providing $(k - k')$ in the range of K_M. Moreover, because the shear instabilities have very little dispersion, the real parts of the frequencies provide $(\omega - \omega') \approx \omega_M$. Thus the Wronskian of the response, $\mathcal{W}([\omega - \omega'] + i[\sigma + \sigma'], [k - k'])$, is close to the line of zeros $\mathcal{W}(\omega_M + i\sigma_M, K_M)$. The lines k, k' used in the previous section met the criteria of large σ, σ' and wavenumber matching $(k - k') = K_M$. The resulting small values of $\mathcal{W}$ provided the efficient response in the upscale scattering. In fact, as long as $(k - k')$ was matched to a long-wavelength modal value, the response stayed large, regardless of how k and k' were manipulated. Some fine tuning was possible, but no really significant variations in overlap integrals or other factors could be detected. However, if the difference $(k - k')$ was allowed to fall outside the modal range K_M, there was no nearby zero of $\mathcal{W}$ and the response was much smaller.

We may thus conclude that the upscale scattering is confined to the wavenumber domain already defined by the results of linearized stability theory. However, within this range the growth rate derived from linear stability theory provides no guide to the nonlinear results. Hence the present results and those of the linear theory agree on the location of the preferred wavenumber domain, and do not necessarily agree on the weighting within it. They certainly do not assign the same time scale to the growth of the long-wavelength disturbance, with the nonlinear theory producing much faster growths.

One final comment on the domain of the preferred response should be made. The first part of this investigation (Chimonas and Grant, 1984) looked at the consequences of introducing destabilizing shear on a small "internal" scale. Comparison of Figs. 2 and 3 of that work reveals that for the more likely Richardson numbers ($J_0 > 0.1$), the two-scale flow allows a much narrower band of unstable gravity-wave wavenumbers than the one-scale flow. In this sense the favored region for upscale scattering can be much more sharply defined in some model flows than in others.

7. The continuum interaction

The previous sections have demonstrated that the upscale scattering of two lines k, k' is effective as long as $(k - k')$ is a wavenumber for a gravity shear wave instability, and both k and k' are strongly represented in the Kelvin–Helmholtz spectrum. We now examine the extension from line theory to continuum theory. Figure 8 is a schematic of the various parts of wavenumber space that are important in this development.

The fields in a continuum of Kelvin–Helmholtz waves have a Fourier representation

$$w_1 = \int_{-\infty}^{\infty} d\omega \int_{-\infty}^{\infty} dk A_{k,\omega}(z) e^{i(\omega t - kx)}, \qquad (7.1)$$

where the reality of the physical fields requires

$$A_{-k,-\omega} = A^*_{k,\omega}. \qquad (7.2)$$

Note that (7.1) is a representation in real ω, k space, and its existence requires certain properties of the field w_1, most noticeably that w_1 is suitably bounded as $|t|$ becomes very large. When the waves are initially instabilities, as in the present case, the boundedness in the time domain comes from nonlinear factors in the dynamics. The $A_{k,\omega}$ will reflect this and, in general, may have very little similarity to any functions derived from linearized theory. However, the representation (7.1) must yield an initial growth phase that resembles linearized theory (assuming *some*

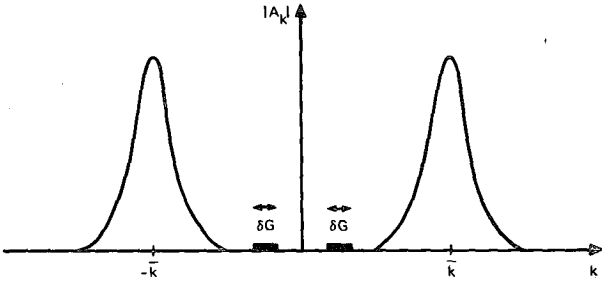

FIG. 8a. Wavenumber space geometry of the waves. The Kelvin–Helmholtz waves center on wavenumbers $\pm\bar{k}$, and their spectral shape half-widths are W. The gravity shear modes are located in the domain bands δG.

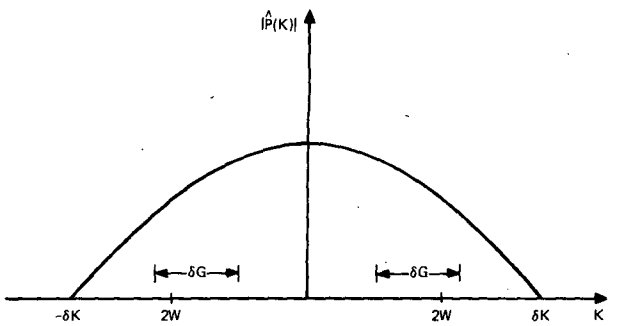

FIG. 8b. The packet width and the gravity shear mode domain. The Kelvin–Helmholtz packet envelope has a spectrum centered on $K = 0$ and a half-width of $2W$. Upscale scattering requires that the domain δG lies between $K = 0$ and δK, where δK is the other limit of the envelope packet, typically a few times W.

relevance of that body of work). As the present calculations are solely concerned with dynamics in that initial phase, a more specialized representation can be used. This is simply the linearized representation

$$w_1 = \int_{-\infty}^{\infty} dk A_k \phi_k(z) e^{\sigma t + i(\omega t - kx)}, \tag{7.3}$$

$$A_{-k} = A_k^*, \quad \omega(-k) = -\omega(k), \quad \phi_{-k} = \phi_k^*, \tag{7.4}$$

valid as a reasonable approximation to (7.1) for some initial time interval $t < T$. The ω integration in (7.1) provides the simplified t-dependence of (7.3) for small (t/T), at least in theory. With this approximation, the nonlinear products $\mathbf{F}_2$ and Q_2 of the set (3.6)–(3.8) take the form of double integrals. Thus

$$\mathbf{F}_2 = Op \int_{-\infty}^{\infty} \int_{-\infty}^{\infty} dk dk' A_k A_{k'} \mathcal{J}(\phi_k, \phi_{k'}) \times e^{(\sigma+\sigma')t + i(\omega+\omega')t - i(k+k')x}. \tag{7.5}$$

The operator Op extracts the long wavelength part of the expression. In the line approximation, this was accomplished by examining the terms (4.2) and (4.3). A similar procedure is still possible. We assume that the Kelvin–Helmholtz amplitudes A are peaked around wavenumbers $|k|$ that are at least an order of magnitude larger than the wavenumbers of the gravity waves. Then, using (7.4) to reform (7.5),

$$\mathbf{F}_2 = Op \int_0^{\infty} \int_0^{\infty} dk dk' \{A_k A_{k'} \mathcal{J}(\phi_k, \phi_{k'}) \exp[(\sigma + \sigma')t + i(\omega + \omega')t - i(k + k')x] + A_k A_{k'}^* \mathcal{J}(\phi_k, \phi_{k'}^*) \times \exp[(\sigma + \sigma')t + i(\omega - \omega')t - i(k - k')x]\} + \text{c. c.}, \tag{7.6}$$

The first term within braces has a wavenumber at least twice as large as some waves in the Kelvin–Helmholtz spectrum, while the second term contains the long wavelengths. Accordingly,

$$\mathbf{F}_2 = \int_0^{\infty} \int_0^{\infty} dk dk' A_k A_{k'}^* \mathcal{J}(\phi_k, \phi_{k'}^*) \times e^{(\sigma+\sigma')t + i(\omega-\omega')t - i(k-k')x} + \text{c. c.} \tag{7.7}$$

Expression (7.7) could be evaluated numerically, and some comparison with the line strengths devised. We prefer to attempt an analytic investigation using properties of idealized wave packets. Deductions from such an approach must be used carefully. For some laboratory situations the packet approach yields accurate quantitative results, but in less controlled environments its predictions have only limited value, mainly providing qualitative evaluation of the factors involved.

With this explicit warning, we offer a very idealized wave packet analysis. In the present problem, packet properties are most conveniently defined through the square of the vertical velocity fluctuations. From (7.3),

$$|w_1|^2 = \int_0^{\infty} \int_0^{\infty} dk dk' A_k A_{k'}^* \phi_k(z) \times \phi_{k'}^*(z) e^{(\sigma+\sigma')t + i(\omega-\omega')t - i(k-k')x}. \tag{7.8}$$

Now suppose that A_k is nonzero only in the small intervals of width $2\delta k$ centered about $\pm\bar{k}$. Then (7.8) may be reformed as

$$|w_1|^2 = \int_{\bar{k}-\delta k}^{\bar{k}+\delta k} dk \int_{\bar{k}-\delta k}^{\bar{k}+\delta k} dk' \{A_k A_{k'}^* \phi_k \phi_{k'}^* e^{i[(\omega-\omega')t - (k-k')x]} + A_k A_{k'} \phi_k \phi_{k'} e^{i[(\omega+\omega')t - (k+k')x]}\} e^{(\sigma+\sigma')t} + \text{c. c.}, \tag{7.9}$$

or, defining a local group velocity

$$v_g = \left.\frac{\partial \omega}{\partial k}\right|_{\bar{k}},$$

$$|w_1|^2 \approx \int_{\bar{k}-\delta k}^{\bar{k}+\delta k} dk \int_{\bar{k}-\delta k}^{\bar{k}+\delta k} dk' \{A_k A_{k'}^* \phi_k \phi_{k'}^* e^{i(v_g t - x)(k-k')} + A_k A_{k'} \phi_k \phi_{k'} e^{i(\omega+\omega')t - (k+k')x}\} e^{2\bar{\sigma}t} + \text{c. c.} \tag{7.10}$$

The second term within the braces of (7.10) is rapidly oscillating. It can be expressed as a slowly varying packet of waves with frequency $2\bar{\omega}$, but its local contribution averaged over a few wave cycles is very small. The first term, on the other hand, is entirely slowly varying. It is the envelope of the mean square velocity field, and we will use it to define the packet shape $P(x - v_g t)$:

$$\langle |w_1|^2 \rangle = P(x - v_g t) |\phi_{\bar{k}}|^2 e^{2\bar{\sigma}t}, \tag{7.11}$$

where

$$P(x) = \int_{\bar{k}-\delta k}^{\bar{k}+\delta k} dk \int_{\bar{k}-\delta k}^{\bar{k}+\delta k} dk' A_k A_{k'}^* e^{-i(k-k')x} + \text{c. c.} \tag{7.12}$$

The double integration can be reformulated as

$$P(x) = \int_{-2\delta k}^{2\delta k} dk \exp - iKx \int_{\bar{k}-\delta k}^{\bar{k}+\delta k} dsA_{(1/2)(s+k)}A^*_{(1/2)(s-k)} + \text{c. c.} \quad (7.13)$$

This shows how the Fourier representation of the packet shape is related to the Kelvin–Helmholtz spectrum

$$P(x) = \int_{-2\delta k}^{2\delta k} dK\hat{P}(K)e^{-iKx} + \text{c. c.}, \quad (7.14)$$

with

$$\hat{P}(K) = \int_{\bar{k}-\delta k}^{\bar{k}+\delta k} dsA_{(1/2)(s+k)}A^*_{(1/2)(s-k)}. \quad (7.15)$$

These results may be used to evaluate (7.7). In the same wave packet approximations,

$$\mathbb{F}_2 = \int_{-2\delta k}^{2\delta k} dke^{i(v_g t-x)k+2\bar{\sigma}t} \int_{\bar{k}-\delta k}^{\bar{k}+\delta k} dsA_{(1/2)(s+k)}A^*_{(1/2)(s-k)} \times (\phi_{(1/2)(s+k)}, \phi^*_{(1/2)(s-k)}) + \text{c. c.} \quad (7.16)$$

The other forcing term Q_2 of (3.8) can be put into an identical form.

The line calculations correspond to a Kelvin–Helmholtz spectrum of two delta functions:

$$A_k|_{\text{line}} = w_1\delta(k - k_1) + w_2\delta(k - k_2), \quad (7.17)$$

so that

$$\mathbb{F}_2|_{\text{line}} = w_1w_2^*\mathcal{F}(\phi_{k_1}, \phi^*_{k_2})e^{i(v_g t-x)(k_1-k_2)+2\bar{\sigma}t} + \text{c. c.} \quad (7.18)$$

The long wavelength response is governed by a linear inhomogeneous equation, with $\mathbb{F}_2$ defining the inhomogeneity. However, the solution of such an equation with a sum of inhomogeneous terms is the sum of the responses to each of the inhomogeneous terms. So the response to the continuum forcing $\mathbb{F}_2$ is the integral over K and s of the response to the integrand in (7.16). This is, within the normalization factors, the response in the corresponding line problem (7.18). It is now possible to make an explicit evaluation of the continuum response using the results of line theory. It was mentioned in Section 6 that the response is insensitive to the particular choice of the Kelvin–Helmholtz lines that provide a given wavenumber difference $k - k' = K$. Moreover, the main dependence on K came from whether or not K lay inside the domain of the gravity shear modes.

We approximate these findings by setting the response to be zero if the wave number K is outside the domain of the modes, and to a constant if it is inside this domain. Then (7.16) leads to

$$\text{Continuum response} = \int_{\text{wavenumbers}}^{\text{modal}} dKe^{i(v_g t-x)K+2\bar{\sigma}t} \times A_{(1/2)(s+K)}A^*_{(1/2)(s-K)}R_{\text{line}} + \text{c. c.} \quad (7.19)$$

The constant R_{line} is a line response with $w_1w_2^*$ in (7.18) set to unity. (The reported responses of Section 5 took $w_1w_2^*$ to be 10^{-2} m^2 s^{-2}.) Using (7.15),

$$\text{Continuum response} = R_{\text{line}} \int_{\text{wavenumbers}}^{\text{modal}} dK\hat{P}(K) \times \exp[i(v_g t - x)K + 2\bar{\sigma}t] + \text{c. c.} \quad (7.20)$$

So, for the idealized wave packet, the continuum response is related to the line response by the fraction of the packet that corresponds to gravity shear-mode wavenumbers.

Figure 8 summarizes the wavenumber space relationships. It is immediately seen from this figure that if the domain δG of the gravity waves lies at wavenumbers greater than δK, the bounds of the wave packet, there is no overlap and (7.20) is zero. There is an inverse relation between the physical dimension of a wave packet and its width in K space, and the above result simply states that if the length of the Kelvin–Helmholtz wave train is very large compared with the wavelengths of the gravity shear modes, no gravity waves can be excited. This is a rather obvious conclusion and an unlikely physical situation. Another limit can be obtained when the width δG of the gravity mode domain is considerably less than the packet width δK. In this case the gravity wave response will extend over a much wider horizontal distance than the packet: a gravity wave "line" has been excited by the "localized" Kelvin–Helmholtz disturbance. This is likely to be a common circumstance where regions of shear instability break into local activity involving a limited number of wave cycles. But now the amplitude of the excitation is small because only a limited range of combinations within the Kelvin–Helmholtz spectrum matches the gravity shear mode domain. Roughly estimating (7.20), this situation produces

$$\int_{\text{wavenumbers}}^{\text{modal}} dK\hat{P}(K)e^{i(v_g t-x)K+2\bar{\sigma}t} \approx \frac{\delta G}{\delta K}\exp[i(v_g t - x)K_G + 2\bar{\sigma}t]\int dK\hat{P}(K), \quad (7.21)$$

so

$$\text{Continuum response} = \left(\frac{\delta G}{\delta K}\right)\langle|w_1|^2\rangle R_{\text{line}}. \quad (7.22)$$

If the disturbance at the center of the packet reaches amplitude $\langle w_1^2\rangle$, the response is equal to that calculated for the two lines, each of strength $(\langle w_1^2\rangle)^{1/2}$, reduced by a factor $(\delta G/\delta K)$. This reduction factor

can be very severe and indicates the need to treat the predictions of line theory with caution. Our line calculations suggested that the gravity waves could easily be excited by interactions among the Kelvin–Helmholtz waves. The lines and their strengths were arbitrarily specified to present the most impressive version of the theory. In the atmosphere, however, the Kelvin–Helmholtz packet will not arrange itself to the benefit of any particular version of a theory. The continuum formulation shows that only a subset of possible packets can produce excitations that are within an order of magnitude of the more optimistic interpretations of line theory. Finally, really efficient packets for the upscale scattering process will be quite rare, as several conditions must be simultaneously satisfied. The packet length L would ideally match a wavelength $2\pi/K_G$ near the center of the gravity mode domain ($K_G L \approx 1$), and this domain should have a width ΔK comparable with K_G. Present observations of the atmosphere are too sparse to allow assignment of statistics to such conditions, but we do not expect them to be common. On the other hand, the efficiency of the favored lines is so high that a sizeable gravity wave results from moderate Kelvin–Helmholtz line strengths, off-setting some of the negative aspects introduced by the continuum. Theoretically, the upscale scattering process could be much more effective than direct generation by the linear shear instability. The process should be regarded as a serious candidate for the interpretation of gravity shear waves that appear to emanate from a region of strong wind shear. But this theory cannot be set in an atmospheric perspective until detailed observations of the spatial extent of Kelvin–Helmholtz disturbances are made.

Acknowledgments. This work was funded by NOAA during 1978–80 while GC was employed by the Wave Propagation Laboratory and JRG was a graduate student at CIRES. It was completed with support from the National Science Foundation under grant ATM-8317367.

APPENDIX

The Forcing Function E_2

The procedures outlined in Sections 1–4 led to the inhomogeneous differential equation (4.7) with a forcing function $E_2(q_k, q_{k'})$. The derivation of (4.7) from the basic equations (3.6)–(3.8) is direct but algebraically tedious. The low phase velocity approximation $(c_x/C)^2 \ll 1$ is assumed, giving

$$E_2(q_k, q_{k'}) = \alpha_2\Omega_2^{-1}[i\alpha_2\rho_0^{-1/2}\mathcal{F}_z + (\rho_0^{-1/2}\mathcal{F}_x)'] - [C^2\rho_0^{-1/2}Q]' - \alpha_2^2 JQC^2\rho_0^{-1/2}\Omega_2^{-2} - \alpha_2 U'C^2\rho_0^{-1/2}Q\Omega_2^{-1}. \quad \text{(A1)}$$

The notation is defined in Sections 2–4 and

$$\mathbf{F}_2 = -\rho_0\mathbf{V}_1\cdot\nabla\mathbf{V}_1 = (\bar{x}\mathcal{F}_x + \bar{z}\mathcal{F}_z)\exp[i(\omega - \omega')t - i(k - k')x + (\sigma + \sigma')t], \quad \text{(A2)}$$

$$Q_2 = \mathbf{V}_1\cdot\nabla p_1 = Q\exp[i(\omega - \omega')t - i(k - k')x + (\sigma + \sigma')t]. \quad \text{(A3)}$$

REFERENCES

Chimonas, G., and J. R. Grant, 1984: Shear excitation of gravity waves. Part I: Modes of a two-scale atmosphere. *J. Atmos. Sci.*, **41**, 2269–2277.

Davis, P. A., and W. R. Peltier, 1976: Resonant parallel shear instability in the stably stratified boundary layer. *J. Atmos. Sci.*, **33**, 1287–1300.

——, and ——, 1977: Effects of dissipation on parallel shear instability near the ground. *J. Atmos. Sci.*, **34**, 1868–1884.

——, and ——, 1979: Some characteristics of Kelvin–Helmholtz and resonant overreflection modes of shear flow instability and their interaction through vortex pairing. *J. Atmos. Sci.*, **36**, 2394–2412.

Fritts, D. C., 1982: Shear excitation of atmospheric gravity waves. *J. Atmos. Sci.*, **39**, 1936–1952.

——, 1984: Shear excitation of atmospheric gravity waves. Part II: Nonlinear radiation from a free shear layer. *J. Atmos. Sci.*, **41**, 524–537.

Herron, T. J., and I. Tolstoy, 1969: Tracking jetstream winds from ground level pressure signals. *J. Atmos. Sci.*, **26**, 266–269.

Hooke, W. H., and K. R. Hardy, 1975: Further study of the atmospheric gravity waves over the Eastern Seaboard on 18 March 1969. *J. Appl. Meteor.*, **14**, 31–38.

——, F. F. Hall, Jr. and E. E. Gossard, 1973: Observed generation of an atmospheric gravity wave by shear instability in the mean flow of the planetary boundary layer. *Bound.-Layer Meteor.*, **5**, 29–41.

Jones, W. L., 1968: Reflection and stability of waves in stably stratified fluids with shear flow: A numerical study. *J. Fluid Mech.*, **34**, 609–624.

Keliher, T. E., 1975: The occurrence of microbarograph-detected gravity waves compared with the existence of dynamically unstable wind shear layers. *J. Geophys. Res.*, **80**, 2967–2976.

Lalas, D. P., and F. Einaudi, 1976: On the characteristics of gravity waves generated by atmospheric shear layers. *J. Atmos. Sci.*, **33**, 1248–1259.

Longuet-Higgins, M. S., 1950: A theory of the origin of microseisms. *Proc. Roy. Soc. London*, **A243**, 857–892.

McIntyre, M. E., and M. A. Weissman, 1978: On radiating instabilities and resonant overreflection. *J. Atmos. Sci.*, **35**, 1190–1196.

Mastrantonio, G., F. Einaudi, D. Fua and D. P. Lalas, 1976: Generation of gravity waves by jet streams in the atmosphere. *J. Atmos. Sci.*, **33**, 1730–1738.

Merrill, J. T., 1977: Observational and theoretical study of shear instability in the air flow near the ground. *J. Atmos. Sci.*, **34**, 911–921.

Metcalf, J. I., and D. Atlas, 1973: Microscale ordered motions and atmospheric structure associated with thin echo layers in stably stratified zones. *Bound.-Layer Meteor.*, **4**, 7–36.

Patnaik, P. C., F. S. Sherman and G. M. Corcos, 1976: A numerical simulation of Kelvin–Helmholtz waves of finite amplitude. *J. Fluid Mech.*, **73**, 215–240.

Rosenthal, A. J., and R. S. Lindzen, 1983: Instabilities in a stratified fluid having one critical level. Part II: Explanation of gravity wave instabilities using the concept of overreflection. *J. Atmos. Sci.*, **40**, 521–529.

Scotti, R. S., and G. M. Corcos, 1972: An experiment on the stability of small disturbances in a stratified free shear layer. *J. Fluid Mech.*, **52**, 499–528.